Fast Numerical Modeling of Multitransmitter Electromagnetic Data Using Multigrid Quasi-Linear Approximation

Takumi Ueda and Michael S. Zhdanov

***Abstract*—Multitransmitter electromagnetic (EM) surveys are widely used in remote-sensing and geophysical exploration. The interpretation of the multitransmitter geophysical data requires numerous three-dimensional (3-D) modelings of the responses of the receivers for different geoelectrical models of complex geological formations. In this paper, we introduce a fast method for 3-D modeling of EM data, based on a modified version of quasilinear approximation, which uses a multigrid approach. This method significantly speeds up the modeling of multitransmitter-multi-receiver surveys. The developed algorithm has been applied for the interpretation of marine controlled-source electromagnetic (MCSEM) data. We have tested our new method using synthetic problems and for the simulation of MCSEM data for a geoelectrical model of a Gemini salt body.**

***Index Terms*—Electromagnetic (EM), multigrid approach, multitransmitter modeling, quasilinear (QL) approximation.**

I. Introduction

Many geophysical electromagnetic (EM) methods use multitransmitter and multireceiver surveys for studying the earth interior. For example, there is a growing interest in marine controlled-source electromagnetic (MCSEM) surveys for petroleum exploration [1]. These surveys are based on using array sea-bottom receivers and moving horizontal electric dipole (HED) transmitters. The seafloor electrodes measure the low-frequency (the frequency range is typically from 0.1–10 Hz) electrical field generated by the HED source transmitting from different positions. An observational survey consists of many transmitters and receivers located over the examined sea-bottom area; both the amplitude and the phase of electric field is measured in the receivers. The goal of these surveys is to find the resistive geoelectrical structures within the conductive sea-bottom formations, associated with the petroleum reservoirs, including both geoelectrical and geometrical parameters of the sea-bottom geological formations.

The interpretation of MCSEM data requires numerous three-dimensional (3-D) modelings of the responses in the receivers for different geoelectrical models of complex sea-bottom geological formations. This task may be extremely expensive, even on modern computers and PC clusters. Over the last decade, several approximate methods of EM modeling have been developed, which may help to overcome this problem. These are the extended Born (localized nonlinear) approximation [2], the quasilinear (QL) approximation [3], QL series [4], quasianalytic approximation and quasianalytic series [5], etc. All of these methods represent different extensions of the classical Born approximation method developed originally to describe quantum mechanical scattering [6], [7].

In this paper, we introduce a novel approach to the numerical modeling of multisource data, typical for MCSEM surveys, using the modified QL approximation. To increase the numerical efficiency of the QL method, we use a special form of the QL approximation based on a multigrid approach. In the framework of this approach, we discretize the conductivity distribution in the model and the electric fields using two grids, a coarse discretization grid and a fine discretization grid. The solution of the forward problem consists of two steps. In the first step, we apply a rigorous integral equation (IE) method to determine the EM field on the coarse grid. We use the results of this IE modeling for computing the electrical reflectivity tensor. In the next step, we apply the QL approximation to the field on a fine grid using the interpolated values of the reflectivity tensor computed on the coarse grid. The technique accelerates the computations significantly while maintains the accuracy of the EM modeling.

The developed technique is illustrated by numerical examples of synthetic MCSEM surveys and the simulation of MCSEM data for a geoelectrical model of a Gemini salt body.

II. QL Approximation Using a Multigrid Approach

The QL approximation is based on the IE representation of the Maxwell's equations. In the framework of the IE method, the electric field $\mathbf{E}$ can be computed using the following integral formula [8], [9]

$$\begin{aligned}\mathbf{E}(\mathbf{r}') &= \iiint_D \widehat{\mathbf{G}}_E(\mathbf{r}' \mid \mathbf{r}) \cdot [\Delta\sigma(\mathbf{r})\mathbf{E}(\mathbf{r})]dv + \mathbf{E}^b(\mathbf{r}') \\ &= \mathbf{G}_E[\Delta\sigma(\mathbf{r})\mathbf{E}(\mathbf{r})] + \mathbf{E}^b(\mathbf{r}') \qquad (1)\end{aligned}$$

where $\widehat{\mathbf{G}}_E(\mathbf{r}_j \mid \mathbf{r})$ is the electric Green's tensor defined for an unbounded conductive medium with the background conductivity σ_b; $\mathbf{G}_E$ is the corresponding Green's linear operator; and domain D corresponds to a volume with the anomalous conductivity distribution $\sigma(\mathbf{r}) = \sigma_b + \Delta\sigma(\mathbf{r})$, $\mathbf{r} \in D$. The total electric field is represented as a sum of the anomalous $\mathbf{E}^a$ and background $\mathbf{E}^b$ fields

$$\mathbf{E}(\mathbf{r}) = \mathbf{E}^a(\mathbf{r}) + \mathbf{E}^b(\mathbf{r}).$$

Manuscript received July 25, 2005; revised November 23, 2005.

The authors are with the Geology and Geophysics Department, University of Utah, Salt Lake City, UT 84112 USA (e-mail: mzhdanov@mines.utah.edu).

Digital Object Identifier 10.1109/TGRS.2006.864386

The QL approximation is based on the assumption that the anomalous field $\mathbf{E}^a$ inside the inhomogeneous domain is linearly proportional to the background field $\mathbf{E}^b$ through some tensor $\widehat{\boldsymbol{\lambda}}$ [10]

$$\mathbf{E}^a(\mathbf{r}) \approx \widehat{\boldsymbol{\lambda}}(\mathbf{r}) \cdot \mathbf{E}^b(\mathbf{r}). \tag{2}$$

Substituting formula (2) into (1), we obtain the QL approximation $\mathbf{E}^a_{QL}(\mathbf{r})$ for the anomalous field

$$\mathbf{E}^a_{QL}(\mathbf{r}_j) = \mathbf{G}_E\left[\Delta\sigma(\mathbf{r})\left(\widehat{\mathbf{I}} + \widehat{\boldsymbol{\lambda}}(\mathbf{r})\right) \cdot \mathbf{E}^b(\mathbf{r})\right]. \tag{3}$$

The last formula for $\mathbf{r}_j \in D$ gives us *the tensor quasilinear (TQL) equation* with respect to the electrical reflectivity tensor $\widehat{\boldsymbol{\lambda}}$ [11]

$$\widehat{\boldsymbol{\lambda}}(\mathbf{r}_j) \cdot \mathbf{E}^b(\mathbf{r}_j) = \mathbf{G}_E\left[\Delta\sigma(\mathbf{r})\widehat{\boldsymbol{\lambda}}(\mathbf{r}) \cdot \mathbf{E}^b(\mathbf{r})\right] + \mathbf{E}^B(\mathbf{r}_j) \tag{4}$$

where $\mathbf{E}^B(\mathbf{r}_j)$ is the Born approximation

$$\mathbf{E}^B(\mathbf{r}_j) = \iiint_D \widehat{\mathbf{G}}_E(\mathbf{r}_j \mid \mathbf{r}) \cdot \left[\Delta\sigma(\mathbf{r})\mathbf{E}^b(\mathbf{r})\right] dv \tag{5}$$

and $\mathbf{G}_E\left[\Delta\sigma(\mathbf{r})\widehat{\boldsymbol{\lambda}}(\mathbf{r}) \cdot \mathbf{E}^b(\mathbf{r})\right]$ is a linear operator of $\widehat{\boldsymbol{\lambda}}(\mathbf{r})$

$$\mathbf{G}_E\left[\Delta\sigma(\mathbf{r})\widehat{\boldsymbol{\lambda}}(\mathbf{r}) \cdot \mathbf{E}^b(\mathbf{r})\right] = \iiint_D \widehat{\mathbf{G}}_E(\mathbf{r}_j \mid \mathbf{r}) \cdot \left[\Delta\sigma(\mathbf{r})\widehat{\boldsymbol{\lambda}}(\mathbf{r}) \cdot \mathbf{E}^b(\mathbf{r})\right] dv. \tag{6}$$

The original QL approximation, introduced by [3], is based on the numerical solution of a minimization problem arising from the TQL (4)

$$\left\|\widehat{\boldsymbol{\lambda}}(\mathbf{r}_j) \cdot \mathbf{E}^b(\mathbf{r}_j) - \mathbf{G}_E\left[\Delta\sigma(\mathbf{r})\widehat{\boldsymbol{\lambda}}(\mathbf{r}) \cdot \mathbf{E}^b(\mathbf{r})\right] - \mathbf{E}^B(\mathbf{r}_j)\right\| = \min. \tag{7}$$

The advantage of this approach is that we can determine the electrical reflectivity tensor $\widehat{\boldsymbol{\lambda}}$ by solving a minimization problem (7) on a coarse grid. The accuracy of the QL approximation depends only on the accuracy of this discretization of $\widehat{\boldsymbol{\lambda}}$, and, in principle, can be made arbitrarily good.

In essence, this means that we can apply the multigrid approach in the framework of the QL approximation. We discretize the conductivity distribution in the model and the electric fields using two grids, $\sum_c$ and $\sum_f$, where $\sum_c$ is a coarse discretization grid and $\sum_f$ is a fine discretization grid, where each block of the original grid $\sum_c$ is divided into additional smaller cells. First, we solve IE (1) on a coarse grid to determine the total electric field $\mathbf{E}$ using the complex generalized minimal residual method (CGMRM) [11]. After that, we can find the anomalous field $\mathbf{E}^a$ on the coarse grid $\sum_c$

$$\mathbf{E}^a(\mathbf{r}_c) = \mathbf{E}(\mathbf{r}_c) - \mathbf{E}^b(\mathbf{r}_c) \tag{8}$$

where $\mathbf{r}_c$ denotes the centers of the cells of the grid $\sum_c$ with the coarse discretization.

The electrical reflectivity coefficients on the coarse grid can be found using (2)

$$\mathbf{E}^a(\mathbf{r}_c) \approx \widehat{\boldsymbol{\lambda}}(\mathbf{r}_c) \cdot \mathbf{E}^b(\mathbf{r}_c). \tag{9}$$

Note that, in the case of a full reflectivity tensor with nine unknown components, the solution of (9) is nonunique. There are several different ways to specify this solution [3]. For example, one can assume that $\widehat{\boldsymbol{\lambda}}(\mathbf{r}_c)$ is a diagonal tensor

$$\widehat{\boldsymbol{\lambda}} = \begin{bmatrix} \lambda_x & 0 & 0 \\ 0 & \lambda_y & 0 \\ 0 & 0 & \lambda_z \end{bmatrix}. \tag{10}$$

In this case, vector equation (9) results in three independent scalar equations for the corresponding components of the electrical fields and the electrical reflectivity tensor

$$E^a_x = \lambda_x E^b_x,\ E^a_y = \lambda_y E^b_y,\ E^a_z = \lambda_z E^b_z. \tag{11}$$

It is easy to solve (11). However, they have one important limitation which restricts the area of practical application of this form of QL approximation. If one of the components of the background field is equal to zero, the corresponding component of the anomalous field has to be equal to zero, as well, which may introduce a significant error in calculation of the anomalous electric field. Indeed, consider the case of a vertically propagating plane EM wave in a simple geoelectrical model of 3-D inhomogeneity located within a horizontally layered background. In this situation, the vertical component of the background field is identically equal to zero, while there exists a significant vertical component of the anomalous electric field in the vicinity of the local inhomogeneity.

This example shows that the multigrid approach outlined above requires a modification of the basic relationship (2) of the QL approximation. In this situation, we have to modify the QL approximation to allow the anomalous current to flow in different directions. The simplest way to solve this problem was introduced by [12] for 3-D EM modeling in anisotropic formations for well-logging applications. It was assumed that the anomalous field is linear proportional to the absolute value of the background field

$$\mathbf{E}^a(\mathbf{r}) \approx \boldsymbol{\lambda}(\mathbf{r})\left|\mathbf{E}^b(\mathbf{r})\right| \tag{12}$$

where $\boldsymbol{\lambda}(\mathbf{r}) = (\lambda_x, \lambda_y, \lambda_z)$ is an electrical reflectivity vector.

In the framework of the QL approximation, we formulate a general forward EM problem so that the anomalous conductivity can be treated as a perturbation from a known background (or "normal") conductivity distribution. The solution of the EM problem in this case contains two parts: 1) the linear part, which can be interpreted as a direct scattering of the source field by the inhomogeneity without taking into account coupling between scattering (excess) currents, and 2) the nonlinear part, which is composed of the combined effects of the anomalous conductivity and the unknown scattered field in the inhomogeneous structure. The QL approximation is based on the assumption that this last part is proportional to the background electric field, which is reflected in (12).

We should note, however, that exact representation (12) always exists because the corresponding electrical reflectivity vector can always be found for any given anomalous and background electric fields. Equation (12) becomes an approximation if we use some approximate method (for example, a multigrid approach introduced in this paper) for evaluation of the electrical reflectivity vector.

In the framework of the multigrid approach, the components of the electrical reflectivity vector on a coarse grid can be found now by direct calculations as

$$\lambda_x(\mathbf{r}_c) = \frac{E_x^a(\mathbf{r}_c)}{|\mathbf{E}^b(\mathbf{r}_c)|} \tag{13a}$$

$$\lambda_y(\mathbf{r}_c) = \frac{E_y^a(\mathbf{r}_c)}{|\mathbf{E}^b(\mathbf{r}_c)|} \tag{13b}$$

$$\lambda_z(\mathbf{r}_c) = \frac{E_z^a(\mathbf{r}_c)}{|\mathbf{E}^b(\mathbf{r}_c)|} \tag{13c}$$

assuming that $\left|\mathbf{E}^b(\mathbf{r}_c)\right| \neq 0$.

After we have found $\boldsymbol{\lambda}(\mathbf{r}_c)$, we introduce a fine discretization grid $\sum_f$ describing the conductivity distribution in the same model. We determine the $\boldsymbol{\lambda}(\mathbf{r}_f)$ values on this new grid by linear interpolation (where $\mathbf{r}_f$ denotes the centers of the cells of the grid $\sum_f$ with fine discretization). We compute the anomalous electric field $\mathbf{E}^a(\mathbf{r}_f)$ in the centers of the cells of the new grid $\sum_f$ with fine discretization using (12)

$$\mathbf{E}^a(\mathbf{r}_f) \approx \boldsymbol{\lambda}(\mathbf{r}_f)\left|\mathbf{E}^b(\mathbf{r}_f)\right|.$$

We can now find the total electric field $\mathbf{E}(\mathbf{r}f)$ on a new grid, as

$$\mathbf{E}(\mathbf{r}_f) = \mathbf{E}^a(\mathbf{r}_f) + \mathbf{E}^b(\mathbf{r}_f). \tag{14}$$

Finally, we compute the observed fields in the receivers using the discrete analog of formula (1) for the grid with fine discretization. We call this multigrid based approach to the QL approximation an MGQL approximation.

III. Comparison Between the Full IE and MGQL Modeling Results

In this section, we will present the results of our numerical study of a new multigrid-based QL approximations. We begin our analysis with a simple synthetic model of a sea-bottom petroleum reservoir and will conclude with a model study of the Gemini Prospect, Gulf of Mexico.

A. Synthetic Model of a Sea-Bottom Petroleum Reservoir

We consider a synthetic model of a sea-bottom petroleum reservoir. Fig. 1 shows a plan view and a vertical cross section of the model. The sea-bottom reservoir is approximated by a thin resistive body located at a depth of 0.5 km below the sea bottom, with a thickness of 0.05 km and a horizontal size of 10 × 5 km. The background model is formed by the horizontally layered formation (see Fig. 1) with the parameters similar to those used by [13]. The resistivity of the reservoir is 50 Ωm. The depth of

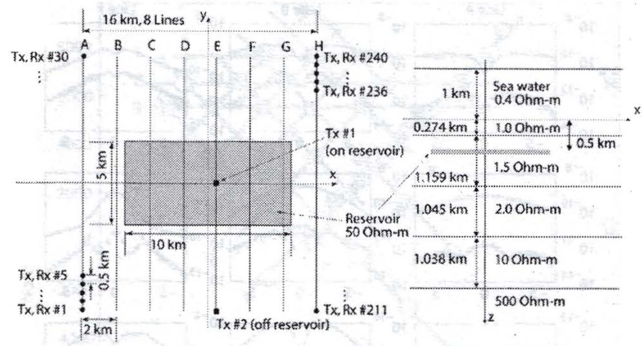

Fig. 1. (Left panel) Plan view and (right panel) a cross section of the synthetic model of a sea-bottom petroleum reservoir and a survey configuration.

the sea bottom is 1 km from the surface, and the sea water resistivity is 0.4 Ωm. The horizontal (y oriented) electric dipole (HED) transmitters have a length of 100 m and are located at a depth 50 m above the sea bottom along eight lines (A, B, C, ... and H) with the separation between the lines equal to 2 km. The distance between the transmitters along each line is 0.5 km. The electric current in the transmitter is 100 A, and the transmitting frequencies are 0.1, 0.2, 0.4, and 1.0 Hz. This set of transmitters simulates an electric bipole transmitter moving along the lines, which is typically used in an MCSEM survey.

The EM field generated by the transmitters is recorded by an array of seafloor electric receivers located 5 m above the sea bottom along the same lines with the same separation between the receivers equal to 0.5 km. In total, there are 240 receivers (30 receivers in each of the eight lines) and 240 positions of the transmitters. The receivers measure the amplitude and the phase of the horizontal and vertical components of the electric field E_x, E_y, and E_z.

In our numerical experiment, we have computed the electric field using two different codes: 1) the forward modeling code INTEM3D based on the rigorous IE method [14] and 2) a new code, INTEM3DQL based on a MGQL approximation, discussed in the previous section.

For numerical modeling, the resistive body was divided into $80 \times 40 \times 4 = 12,800$ cells, with a cell size of $0.125 \times 0.125 \times 0.0125$ km in the x, y, and z directions, respectively. This grid was used for the rigorous IE modeling. We used a coarse grid consisting of $40 \times 20 \times 2 = 1,600$ cells, with a cell size of $0.25 \times 0.25 \times 0.025$ km in the case of the MGQL modeling.

Fig. 2 presents, as an example, the profiles of the absolute values of the electric field components E_x, E_y, and E_z, computed along the lines A, B, and F for a case where the EM field is generated by transmitter #1, located on line E above the center of the reservoir. The frequency of the signal in the transmitter is 0.1 Hz. The top panels in this figure show the absolute values of the total electric field component E_x along the receiver lines A, B, and F. The middle panels present the absolute values of the E_y component, and the bottom panels present the profiles of the E_z component, respectively. In each panel, the solid lines correspond to the data computed using the rigorous IE method, the dotted lines present the MGQL modeling results, the dashed lines show the absolute value of the difference between the IE

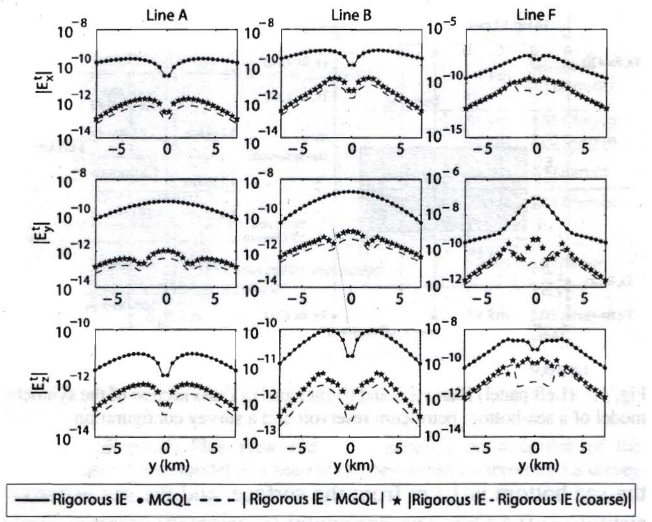

Fig. 2. Profile of three components of the electric field for transmitter #1 (located above the center of the reservoir) at 0.1-Hz along the lines A, B, and F. The solid lines correspond to the data computed using the rigorous IE method. The dotted lines present the MGQL modeling results. The dashed lines show the absolute value of the difference between the IE and MGQL solutions. The stars show the absolute values of the difference between the rigorous IE solutions on a fine and on a coarse grids respectively.

and MGQL solutions, and the stars show the absolute values of the difference between the rigorous IE solutions on a fine and on a coarse grids respectively. One can see that the results obtained by both the IE method and the MGQL approximation fit each other very well. At the same time, the errors produced by the IE solution on the coarse grid (the stars) are larger than the errors of the MGQL approximation (dashed lines).

Fig. 3 (left panels) shows the maps of the different electric field components (absolute values) for the same frequency of 0.1 Hz. The right panels in Fig. 3 present the components of the total electric field normalized by the absolute value of the background electric field in the receivers: $|E_x^t| / |\mathbf{E}^b|$, $|E_y^t| / |\mathbf{E}^b|$, $|E_z^t| / |\mathbf{E}^b|$, respectively. The white lines in the right panels outline the areas where the data are above the measurable signal in the typical sea-bottom receivers' threshold of 10^{-10} V/m. One can notice in this figure that the y component of the electric field, which is parallel to the transmitter orientation, is the strongest one.

Fig. 4 presents the profiles of the absolute values of the E_x, E_y, and E_z components computed along the lines A, B, and F for a case where the EM field is generated by transmitter #2, located on line E outside the reservoir, as shown in Fig. 1. We plot both the rigorous IE and the MGQL results. The maps of the different electric field components (absolute values) for the same frequency of 0.1 Hz are shown in Fig. 5 (left panels), while the right panels in Fig. 5 present the normalized components. It is interesting to notice that for the far field transmitter the magnitudes of all three components become almost of the same order, and a noticeable anomaly appears in the vertical component as well. However, a significant part of the observed data lies in the area outside the threshold level in the receivers. We also analyzed all the data in the receivers collected by a multitransmitter array and measured computational time in order

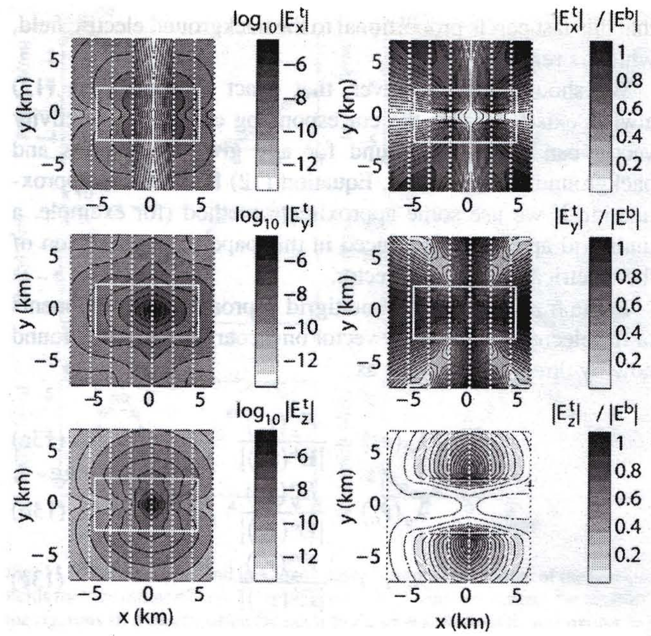

Fig. 3. Two-dimensional maps of electric fields and normalized electric fields for transmitter #1 (located above the center of the reservoir) at 0.1 Hz.

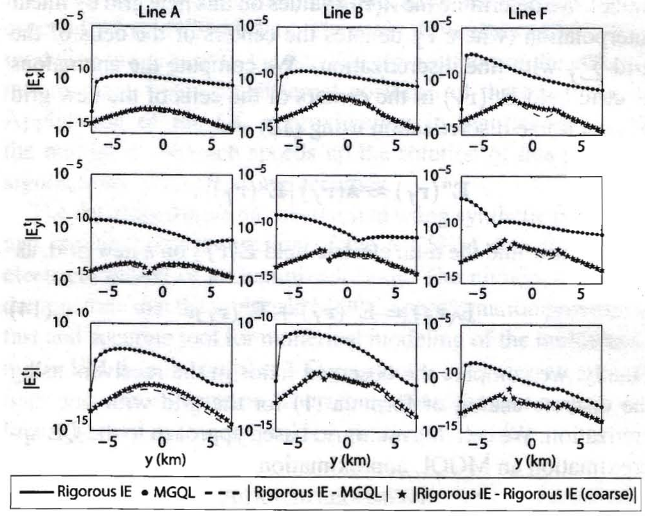

Fig. 4. Profile of three components of the electric field for transmitter #2 (located outside the reservoir) at 0.1 Hz along the lines A, B, and F. The solid lines correspond to the data computed using the rigorous IE method. The dotted lines present the MGQL modeling results. The dashed lines show the absolute value of the difference between the IE and MGQL solutions. The stars show the absolute values of the difference between the rigorous IE solutions on a fine and on a coarse grids, respectively.

to confirm the effectiveness of the MGQL approximation. For the synthetic model described above, the rigorous IE method requires about 150 s for calculation of 240 receivers with one transmitter, whereas it takes about 17 s with the MGQL approximation method. For the computation of 240 receivers and 240 transmitters, the IE method needs about 10 h, whereas the MGQL approximation could finish the job within about an hour. The computer memory required for the IE simulation is equal to 29 MB, while, for the MGQL modeling, we need just 2.3 MB on an AMD Athlon 64, 1.8-GHz PC.

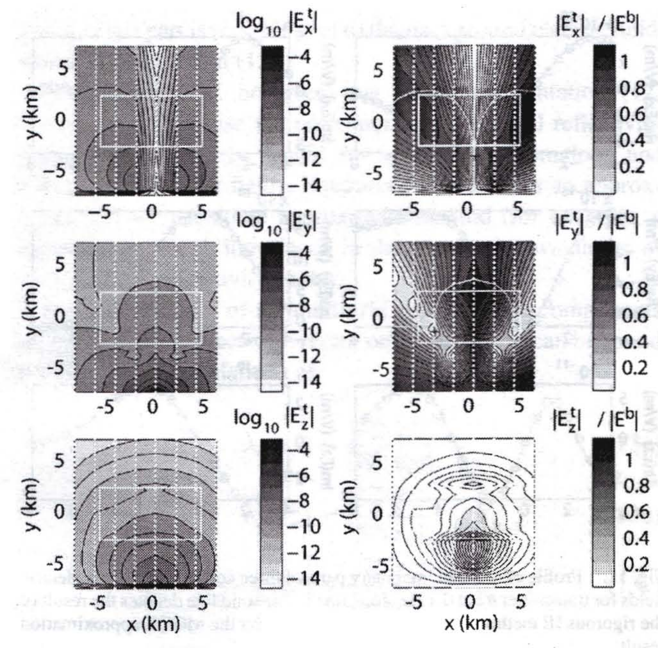

Fig. 5. Two-dimensional maps of electric fields and normalized electric fields for transmitter #2 (located outside the reservoir) at 0.1 Hz.

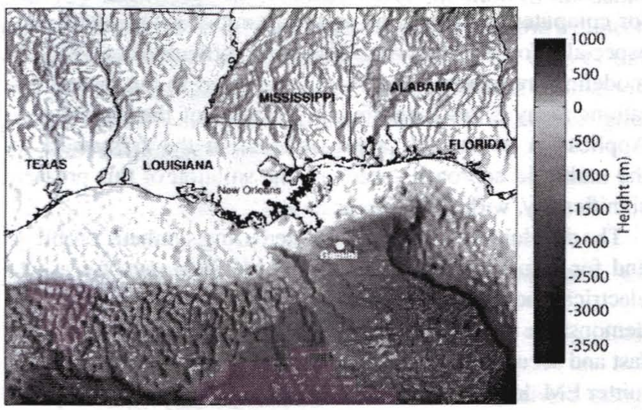

Fig. 6. Location of Gemini Prospect, Gulf of Mexico. Topography and bathymetry from [16].

B. Gemini Prospect Model

We consider a synthetic geoelectrical model of the Gemini Prospect obtained as a result of marine MT data inversion [15].

The Scripps Institution of Oceanography conducted several sea-bottom MT surveys in the Gemini Prospect, Gulf of Mexico, in 1997, 1998, 2001, and 2003, at a total of 42 MT sites [17]. Gemini Prospect lies about 200 km southeast of New Orleans in about 1-km deep water in the northern Gulf of Mexico (Fig. 6). An MT survey was conducted in the Gemini Prospect along several lines shown in Fig. 7 [17], [18]. Zhdanov *et al.*, 2004, conducted a 3-D inversion of the MT data collected at the Gemini prospect [15].

Fig. 8 shows a 3-D image of the volume resistivity distribution in the model, obtained by 3-D inversion. The depth of the sea bottom is 1 km from the surface, and the sea water resistivity is 0.3 Ωm. The horizontal (y oriented) electric dipole (HED) transmitters have a length of 100 m and are located at $(x, y) = (0, 0)$ and $(x, y) = (4, 0)$ km at a depth 50 m

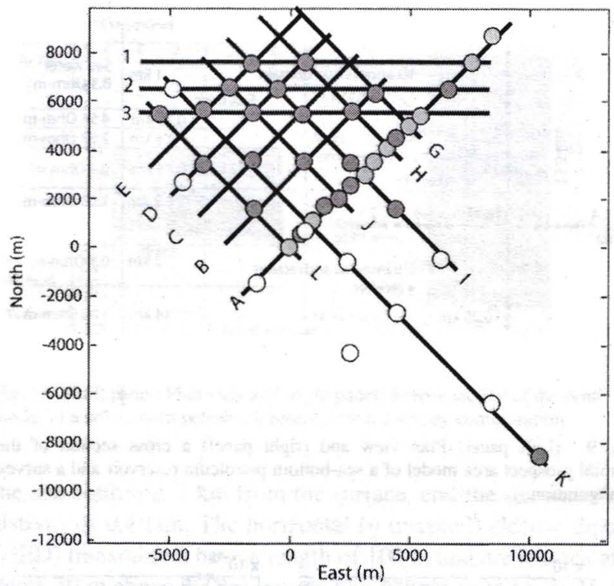

Fig. 7. Location of the MT profiles with the observation sites in Gemini Prospect (after [18]).

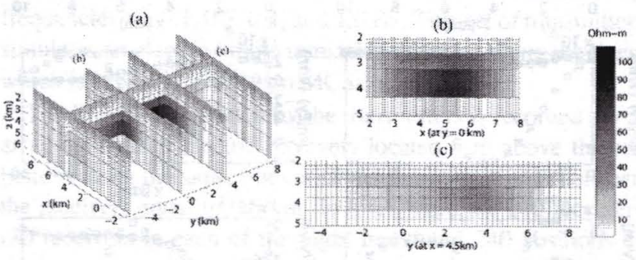

Fig. 8. Three-dimensional image and vetrical cross sections of the geoelectrical model obtained by the MT data inversion [15].

above the sea bottom. They generate an EM field with a transmitting current of 100 A at 0.1 Hz. An array of seafloor electric receivers is located 5 m above the sea bottom along the line A ($x = \{0, 10\}$ km, $y = 0$) and the line I ($x = 4$km, $y = \{-4, 8\}$ km) with a spacing of 0.5 km. For forward modeling, we selected an area of the inversion domain, located at a depth of 2 km below the sea bottom, with a thickness of 4.4 km and a horizontal size of 6.25 × 13.5 km. For the rigorous IE method application, this area was divided into $50 \times 54 \times 10 = 27,000$ cells, with a cell size of $0.125 \times 0.25 \times \{0.1, 0.1, 0.175, 0.175, 0.25, 0.25, 0.5, 0.5, 0.75, 0.75\}$ km in the x, y, and z directions, respectively. In the case of the MGQL approximation, we used $25 \times 27 \times 5 = 3375$ cells, with a cell size of $0.25 \times 0.5 \times \{0.2, 0.25, 0.5, 1.0, 1.5\}$ km. Horizontal and vertical cross sections of the anomalous part of the model and the receiver profiles are shown in Fig. 9 (left panel). The right panel in Fig. 9 presents the background one-dimensional (1-D) layered earth model used in this calculation.

Fig. 10 presents the plots of the real and imaginary E_x, E_y, and E_z components observed along line A due to transmitter #1, located at the center of the profiles (solid lines), and due to transmitter #2, located at the end of the profile (dashed lines). The position of the profiles and the transmitters is shown in Fig. 9. Fig. 11 shows similar plots for profile I. One can see that the

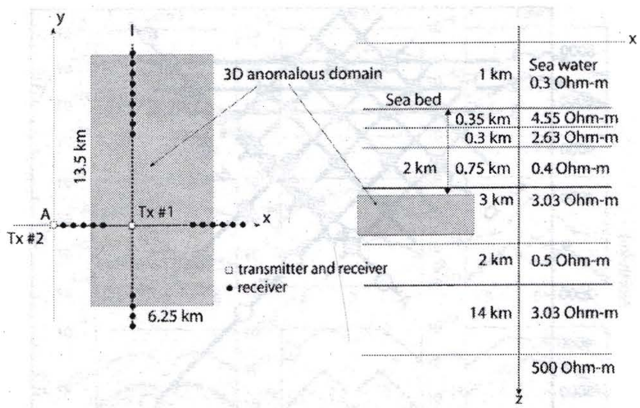

Fig. 9. (Left panel) Plan view and (right panel) a cross section of the Gemini prospect area model of a sea-bottom petroleum reservoir and a survey configuration.

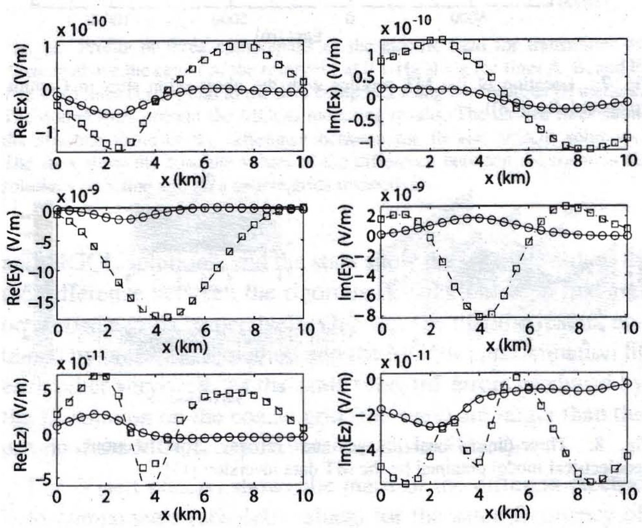

Fig. 10. Profile of real and imaginary parts of three components of the electric fields for transmitters #1 and #2 at 0.1 Hz along line A. The solid line denotes the calculation results for transmitter #1 with the rigorous IE method, while the open circle presents MGQL approximation results. The dashed line is the result for transmitter #2 with the rigorous IE method, while the open square denotes the MGQL approximation results.

plots computed using the rigorous IE method and a MGQL approximation based on the multigrid approach practically coincide, which confirms the accuracy of the new modeling method.

The computational time required for these calculations was 30 s on a 1.8-GHz PC. We should notice that the estimated computation time for the same modeling using the rigorous IE method will be 45 min for a single transmitter and about eight days for 240 transmitters. The computer memory required for the IE simulation is equal to 152 MB, while, for the MGQL modeling, we need just 9.3 MB on an AMD Athlon 64, 1.8-GHz PC.

IV. Conclusion

In this paper, we have developed a new, efficient method of 3-D EM modeling for complex geoelectrical structures based on the multigrid form of the QL approximation. We have

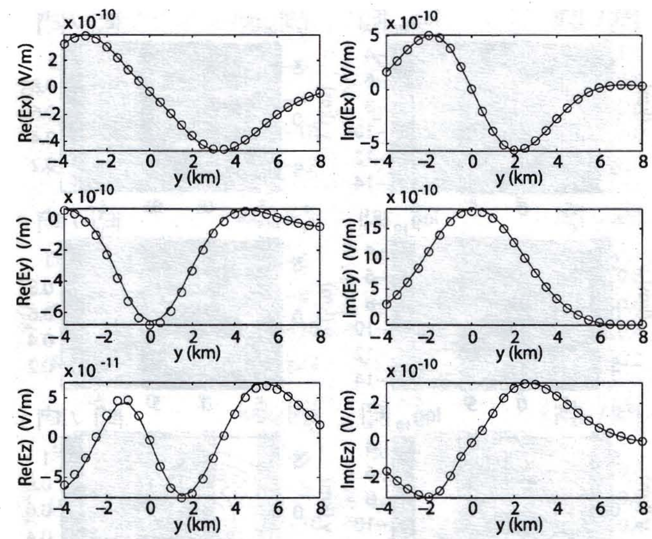

Fig. 11. Profile of real and imaginary parts of three components of the electric fields for transmitter #2 at 0.1 Hz along line I. The solid line denotes the result of the rigorous IE method, while the open circle shows the MGQL approximation result.

demonstrated that this new technique can be effectively used for computer simulation of multitransmitter geophysical data, especially for MCSEM data. The main difficulties of MCSEM modeling are related to the fact that we need to run the computations many times for different positions of the transmitters. Application of the QL approximation in the framework of the multigrid approach speeds up the solution of this problem significantly, without losing accuracy.

The developed code has been tested using synthetic problems and for computer simulation of the MCSEM data for a geoelectrical model of a Gemini salt body. The numerical results demonstrate that the multigrid MGQL approximation provides a fast and accurate tool for numerical modeling of the multitransmitter EM data in complex 3-D geoelectrical structures, typical for petroleum exploration. Therefore, this technique may be effectively used in inverse problem solution as well.

Acknowledgment

The authors would like to thank the University of Utah Consortium for Electromagnetic Modeling and Inversion (CEMI) for their support, including Baker Atlas Logging Services; BGP China National Petroleum Corporation; BHP Billiton World Exploration, Inc.; ENI S.p.A.; ExxonMobil Upstream Research Company; INCO Exploration, Newmont Mining Company; Norsk Hydro; Rio Tinto-Kennecott; Schlumberger; Shell International Exploration and Production, Inc.; Statoil; Sumitomo Metal Mining Company; and Zonge Engineering and Research Organization. They would also like to thank S. Constable and K. Key of the Scripps Institution of Oceanography for providing sea-bottom MT survey parameters.

References

[1] T. Eidesmo, S. Ellingsrud, L. M. MacGregor, S. Constable, M. C. Sinha, S. Johansen, F. N. Kong, and H. Westerdahl, "Sea bed logging (SBL), A new method for remote and direct identification of hydrocarbon filled layers in deepwater areas," *First Break*, vol. 20, pp. 144–152, 2002.

[2] T. M. Habasy, R. W. Groom, and B. R. Spies, "Beyond the Born and Rytov approximations: A nonlinear approach to electromagnetic scattering," *J. Geophys. Res. B*, vol. 98, no. 2, pp. 1759–1775, 1993.
[3] M. S. Zhdanov and S. Fang, "Quasilinear approximation in 3D EM modeling," *Geophyics*, vol. 61, no. 3, pp. 646–665, 1996.
[4] M. Zhdanov and S. Fang, "Quasilinear series in three-dimensional electromagnetic modeling," *Radio Sci.*, vol. 32, no. 6, pp. 2167–2188, 1997.
[5] M. S. Zhdanov, V. I. Dmitriev, S. Fang, and G. Hursan, "Quasianalytical approximation and series in electromagnetic modeling," *Geophysics*, vol. 65, pp. 1746–1757, 2000.
[6] M. Born, *Optik*. Berlin, Germany: Springer, 1933.
[7] M. Born and E. Wolf, *Principles of Optics*. New York: Pergamon, 1980.
[8] G. W. Hohmann, "Three-dimensional induced polarization and EM modeling," *Geophysics*, vol. 40, pp. 309–324, 1975.
[9] P. Weidelt, "EM induction in three-dimensional structures," *J. Geophys.*, vol. 41, pp. 85–109, 1975.
[10] M. S. Zhdanov and S. Fang, "Three-dimensional quasilinear electromagnetic inversion," *Radio Sci.*, vol. 31, no. 4, pp. 741–754, 1996.
[11] M. S. Zhdanov, *Geophysical Inverse Theory and Regularization Problems*. New York: Elsevier, 2002, p. 628.
[12] G. Gao, C. Torres-Verdin, and S. Fang, "Fast 3D modeling of borehole induction measurements in dipping and anisotropic formations using a novel approximation technique," *Petrophysics*, vol. 45, pp. 335–349, 2004.
[13] M. J. Tompkins and R. Weaver, "Methods for the visulaization and interpretation of marine controlled-source electromagnetic data," in *Expand Abstr.*, 2004, Soc. Expl. Geophys., pp. 608–611.
[14] G. Hursán and M. S. Zhdanov, "Contraction integral equation method in three-dimensional electromagnetic modeling," *Radio Sci.*, vol. 37, no. 6, pp. 1089–2002, 2002.
[15] M. S. Zhdanov, L. Wan, S. Constable, and K. Key, "New development in 3-D marine MT modeling and inversion for off-shore petroleum exploration," in *Expanded Abstr.*, 2004, Soc. Expl. Geophys., pp. 588–591.
[16] W. H. F. Smith and D. T. Sandwell, "Global seafloor topography from satellite altimetry and ship depth soundings," *Science*, vol. 277, pp. 1956–1962, 1997.
[17] G. M. Hoversten, S. C. Constable, and H. F. Morrison, "Marine magnetotellurics for base-of-salt mapping: Gulf of Mexico field test at the Gemini structure," *Geophysics*, vol. 65, no. 5, pp. 1476–1488, 2000.
[18] K. W. Key, "Application of Broadband Marine Magnetotelluric Exploration to a 3D Salt Structure and a Fast-Spreading Ridge," Ph.D. dissertation, The Scripps Inst. Oceanography, Univ. California, San Diego, 2003.

Takumi Ueda received the B.Eng. and M.Eng. degrees in geophysics from Waseda University, Tokyo, Japan, in 2000 and 2002, respectively. He is currently pursuing the Ph.D. degree at the University of Utah, Salt Lake City.

Since Fall 2002, he has been with the Consortium for Electromagnetic Modeling and Inversion (CEMI), University of Utah. His current research interests includes 3-D modeling and inversion of the electromagnetic and potential fields and numerical methods for geophysics and scientific computing techniques.

Michael S. Zhdanov received the Ph.D. degree from Moscow State University, Moscow, Russia, in 1970.

He is currently a Professor of geophysics at the University of Utah, Salt Lake City. He spent more than 20 years as a Professor at the Moscow University of Oil and Gas and as the Head of the Department of Deep Electromagnetic Study and Deputy Director of IZMIRAN, and later as Director of the Geoelectromagnetic Research Institute, Russian Academy of Sciences, Moscow, before joining the University of Utah.

Dr. Zhdanov was awarded an Honorary Diploma of Gauss Professorship by the Gottingen Academy of Sciences, Germany, in 1990. In 1991, he was elected Full Member of the Russian Academy of Natural Sciences. He became Honorary Professor of the China National Center of Geological Exploration Technology in 1997 and a Fellow of the Electromagnetics Academy in 2002.